Supplying Baseload Power and Reducing Transmission Requirements by Interconnecting Wind Farms

CRISTINA L. ARCHER AND MARK Z. JACOBSON

Department of Civil and Environmental Engineering, Stanford University, Stanford, California

(Manuscript received 6 July 2006, in final form 6 February 2007)

ABSTRACT

Wind is the world's fastest growing electric energy source. Because it is intermittent, though, wind is not used to supply baseload electric power today. Interconnecting wind farms through the transmission grid is a simple and effective way of reducing deliverable wind power swings caused by wind intermittency. As more farms are interconnected in an array, wind speed correlation among sites decreases and so does the probability that all sites experience the same wind regime at the same time. The array consequently behaves more and more similarly to a single farm with steady wind speed and thus steady deliverable wind power. In this study, benefits of interconnecting wind farms were evaluated for 19 sites, located in the midwestern United States, with annual average wind speeds at 80 m above ground, the hub height of modern wind turbines, greater than 6.9 m s^{-1} (class 3 or greater). It was found that an average of 33% and a maximum of 47% of yearly averaged wind power from interconnected farms can be used as reliable, baseload electric power. Equally significant, interconnecting multiple wind farms to a common point and then connecting that point to a far-away city can allow the long-distance portion of transmission capacity to be reduced, for example, by 20% with only a 1.6% loss of energy. Although most parameters, such as intermittency, improved less than linearly as the number of interconnected sites increased, no saturation of the benefits was found. Thus, the benefits of interconnection continue to increase with more and more interconnected sites.

1. Introduction

Stabilizing global climate, reducing air pollution, and addressing energy shortages will require a change in the current energy infrastructure. One method to address these problems is to initiate a large-scale wind energy program. The world's electric power demand of 1.6–1.8 TW (International Energy Agency 2003; Energy Information Administration 2004) could, for example, theoretically be satisfied with approximately 890 000 currently manufactured 5-MW turbines with 126-m diameter blades placed in yearly averaged wind speeds at hub height of 8.5 m s^{-1} or faster, assuming a 10% loss from energy conversions and transmission (derived from Jacobson and Masters 2001; Masters 2004). This number is only 7–8 times the total number of much smaller turbines currently installed worldwide. The offshore average wind speed at 80 m is 8.6 m s^{-1}, and sufficient winds >6.9 m s^{-1} at 80 m may be available over land and near shores to supply all electric power needs 35 times over and all energy needs 5 times over (Archer and Jacobson 2005).

However, a well known barrier to large-scale implementation of wind power is the intermittency of winds. Over a time frame of a few minutes, it is possible to experience sudden changes in wind speed, such as gusts or lulls. The predictability of wind in the short-term is still low, and, even with elaborate forecasting tools, it is often difficult to beat persistency (Giebel 2003; Ahlstrom et al. 2005). The intermittency of wind is directly transmitted into wind power, which dramatically reduces the marketing value of wind (Milligan and Porter 2005). On the other hand, because coal combustion can be controlled, coal energy is not considered intermittent and is often used as "baseload" energy. Nevertheless, because coal plants were shut down for scheduled maintenance 6.5% of the year and unscheduled maintenance or forced outage for another 6% of the year on average in the United States from 2000 to 2004, coal

Corresponding author address: Cristina L. Archer, Department of Global Ecology, Carnegie Institute of Washington, 260 Panama St., Stanford, CA 94305.
E-mail: lozej@stanford.edu

DOI: 10.1175/2007JAMC1538.1

energy from a given plant is guaranteed only 87.5% of the year, with a typical range of 79%–92% (North American Electric Reliability Council 2005; Giebel 2000).

A solution to improve wind power reliability is interconnected wind power. In other words, by linking multiple wind farms together it is possible to improve substantially the overall performance of the interconnected system (i.e., array) when compared with that of any individual wind farm. The idea is that, while wind speed could be calm at a given location, it will be noncalm somewhere else in the aggregate array.

This idea is not new. The first complete study about the effect of geographically dispersed wind power generation was done by Kahn (1979), who analyzed reliability, availability, and effective load carrying capability [ELCC; see Milligan and Porter (2005) for a review of ELCC] of arrays of different sizes in California, varying from 2 to 13 connected sites. He found that most parameters (such as correlation and availability at low wind speeds) improved as the size of the array increased. Archer and Jacobson (2003, 2004) found that the frequency of zero- and low-wind events over a network of eight sites in the central United States was less than 2% at 80-m hub height. Simonsen and Stevens (2004) compared wind power output from individual wind farms with that from an array of 28 sites in the central United States and concluded that variability in energy production was reduced by a factor of 1.75–3.4. They also found that the combined energy output from 50-m hub height, 660-kW turbines in the 28-site array, had a smoother diurnal pattern and a relative maximum in the afternoon, during the peak time of electricity demand. Czisch and Ernst (2001) showed that a network of wind farms over parts of Europe and Northern Africa could supply about 70% of the entire European electricity demand. In Spain, one of the leading countries for wind power production (American Wind Energy Association 2004; Energy Information Administration 2004), the combined output of 81% of the nation's wind farms is remarkably smooth, and sudden wind power swings are eliminated (Red Eléctrica de España real-time data are available online at http://www.ree.es/apps/i-index_dinamico.asp?menu=/ingles/i-cap07/i-menu_sis.htm&principal=/apps_eolica/curvas2ing.asp).

The benefits of interconnected wind power are greater for larger catchment areas. Statistical correlation among stations is the key factor in understanding why. In fact, weather conditions may not vary over small areas, especially over horizontally uniform terrain. This would be reflected in a high correlation among nearby farm pairs. However, as distance between farms or terrain variability increases, the correlation among farms becomes smaller. Kahn (1979) found that the average correlation between site pairs decreased from 0.49 to 0.25 as the number of farms connected was increased from 2 to 13. However, the marginal benefits decreased as well. For example, by doubling the number of sites connected together, the availability at low wind speeds improved by only ~14%. Whether or not a zero correlation can eventually be reached is still an open question. Kahn (1979) suggested that statistical correlation of wind speed never disappears entirely. This effect will be hereinafter referred to as the "saturation" of the benefits, to indicate that, at some point, no incremental benefits are found in increasing the array size.

Kahn (1979) also analyzed the capacity credit for such arrays, defined as the "amount of conventional capacity which can be displaced by wind generation." He found that, for a fixed ELCC, the capacity credit of larger arrays increased less than linearly with the number of sites. This effect can be interpreted as "diminishing returns to implementing state-wide pooling of the wind resource." Note that of the 13 sites analyzed, only 4 were in class 3 or higher at 60 m. As such, it is not surprising that the addition of "slow" sites to the array did not improve its overall performance.

The issue of wind integration in the power system has been receiving more attention recently (Ackermann 2005; DeMeo et al. 2005; Piwko et al. 2005; Zavadil et al. 2005). Most studies assumed a low (10% or less) penetration of wind power (expressed as ratio of nameplate wind generation over peak load) and treated the output of farms as negative load (Piwko et al. 2005; DeMeo et al. 2005). Only a few countries in Europe have high (20% or more) wind penetrations (Eriksen et al. 2005): Denmark (49%), Germany (22%), and Spain (22%). High penetrations of wind power without reductions in system stability can only be achieved with turbines equipped with fault ride-through capability (Eriksen et al. 2005). No study to date has examined the ability of interconnected wind farms to provide guaranteed (or baseload) power. Only a few studies have looked at reducing transmission requirements by interconnecting wind farms. Romanowitz (2005) reported that an additional 100 MW of wind power could be added to the Tehachapi grid in California without increasing the transmission capacity. Matevosyan (2005) showed that, in areas with limited transmission capacity, curtailing (or "spilling") a small percent of the power produced by interconnected wind farms could be effective. This study examines both issues in detail. It does not, however, examine the ability of wind to match peaks in energy demand. It assumes that wind can pro-

vide a portion of baseload energy, and that peaking energy would be provided by other sources.

2. Interconnected wind power

a. Method

Wind speed data from the National Climatic Data Center (2004) and former Forecast Systems Laboratory (2004), now the Global Systems Division of the Earth System Research Laboratory, for 2000 were used to evaluate the effects of connecting wind farms. More details on the dataset can be found in Archer and Jacobson (2005). Hourly and daily averaged wind speed measurements were available from surface stations at a standard elevation of ~10 m above the ground (V10 hereinafter). Observed vertical profiles of wind speed were available at sounding stations, generally 2 times per day (0000 and 1200 UTC). This study utilized the least squares (LS) method to obtain relevant statistics of wind speed at 80 m (V80 hereinafter), the hub height of modern wind turbines. The reader is referred to Archer and Jacobson (2003, 2004, 2005) for details of the method, which will be further validated in the next section.

To determine wind power output from connected wind farms, the benchmark turbine selected was the GE 1.5 MW with 77-m blade diameter at 80-m hub height. Manufacturer data were provided only at one m s^{-1} intervals of hub height wind speed (General Electric 2004). It was necessary therefore to determine an appropriate curve that would provide power output P for any value of wind speed V. Several multiparameter curves were tried out, including third-order polynomial, sinusoidal, and linear. The best curve was found to be a combination of two third-order polynomials:

$$P = \begin{cases} 0 & V < V_{\text{min}} \\ P_{\text{lower}}(V) & V_{\text{min}} \le V < V_{\text{split}} \\ P_{\text{upper}}(V) & V_{\text{split}} \le V < V_{\text{rated}}, \\ P_{\text{rated}} & V_{\text{rated}} \le V < V_{\text{max}} \\ 0 & V \ge V_{\text{max}} \end{cases} \quad (1)$$

where P_{rated} is the rated power of the turbine (1500 kW) at the rated wind speed V_{rated} (12 m s^{-1}), V_{min} (V_{max}) is the speed below (above) which no power can be produced (3 and 25 m s^{-1}, respectively), V_{split} is the speed above (below) which the P_{upper} (P_{lower}) formulation is imposed (i.e., where the concavity of the power curve changes sign), and P_{upper} and P_{lower} are the third-order polynomials that pass through the upper and lower points of the GE 1.5-MW power curve, respectively:

$$P_i = a_i V^3 + b_i V^2 + c_i V + d_i, \quad i = \text{upper, lower}. \quad (2)$$

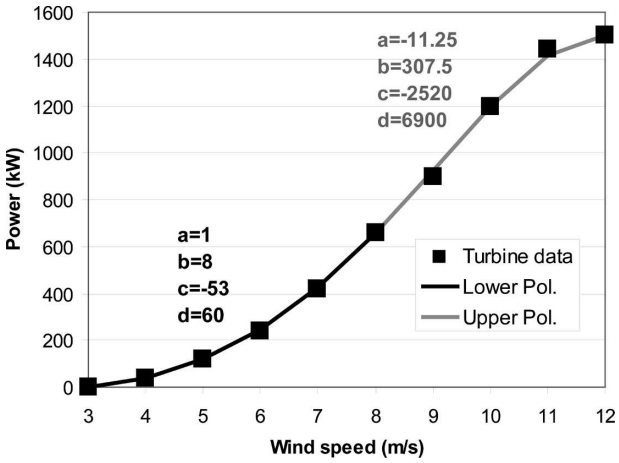

FIG. 1. Fitting curves for the GE 1.5-MW turbine.

Values of the fitting coefficients are reported in Fig. 1. Third-order polynomials were preferred over higher-order curves because of the theoretical dependence of wind power on the third power of wind speed.

Next, the selection of appropriate locations to connect is discussed. From Archer and Jacobson (2003), the central United States was identified as a favorable area for locating and connecting wind farms. Also, locations with mean annual 80-m wind speed > 6.9 m s^{-1} (i.e., in class 3 or higher) were recommended. As such, this study focused on the area shown in Fig. 2.

The LS method was first applied to daily averages of V10 at all surface stations in the area to obtain the spatial distribution of yearly average V80 (hourly data will be used next). LS parameters were calculated from the sounding stations 2 times per day, at 0000 and 1200 UTC, corresponding to 0500–1700 LST, for the entire year 2000. Figure 2 shows annual averages of V80 at sites favorable for harnessing wind power (in class 3 or higher) in the region. The stations selected for the rest of this analysis are listed in Table 1 and marked with their acronyms in Fig. 2. The selection proceeded by enlarging the area around Dodge City, Kansas, the site selected as representative of a single farm.

To determine the differences in power output for individual versus connected wind sites, hourly observed 10-m wind speeds were used to calculate the hourly evolution of V80 via the so-called shear function, described later in section 2b. Last, the hourly power output at each station was calculated with Eq. (1) and averaged over N stations, where N was either 1, 3, 7, 11, 15, or 19. Sites that had missing data at a given hour were not counted in the average for that hour. The frequency of missing data was surprisingly large, about 10%. Given a pool of 19 sites and an array size of K (where K = 1, 3, 7, 11, 15, or 19), the number of pos-

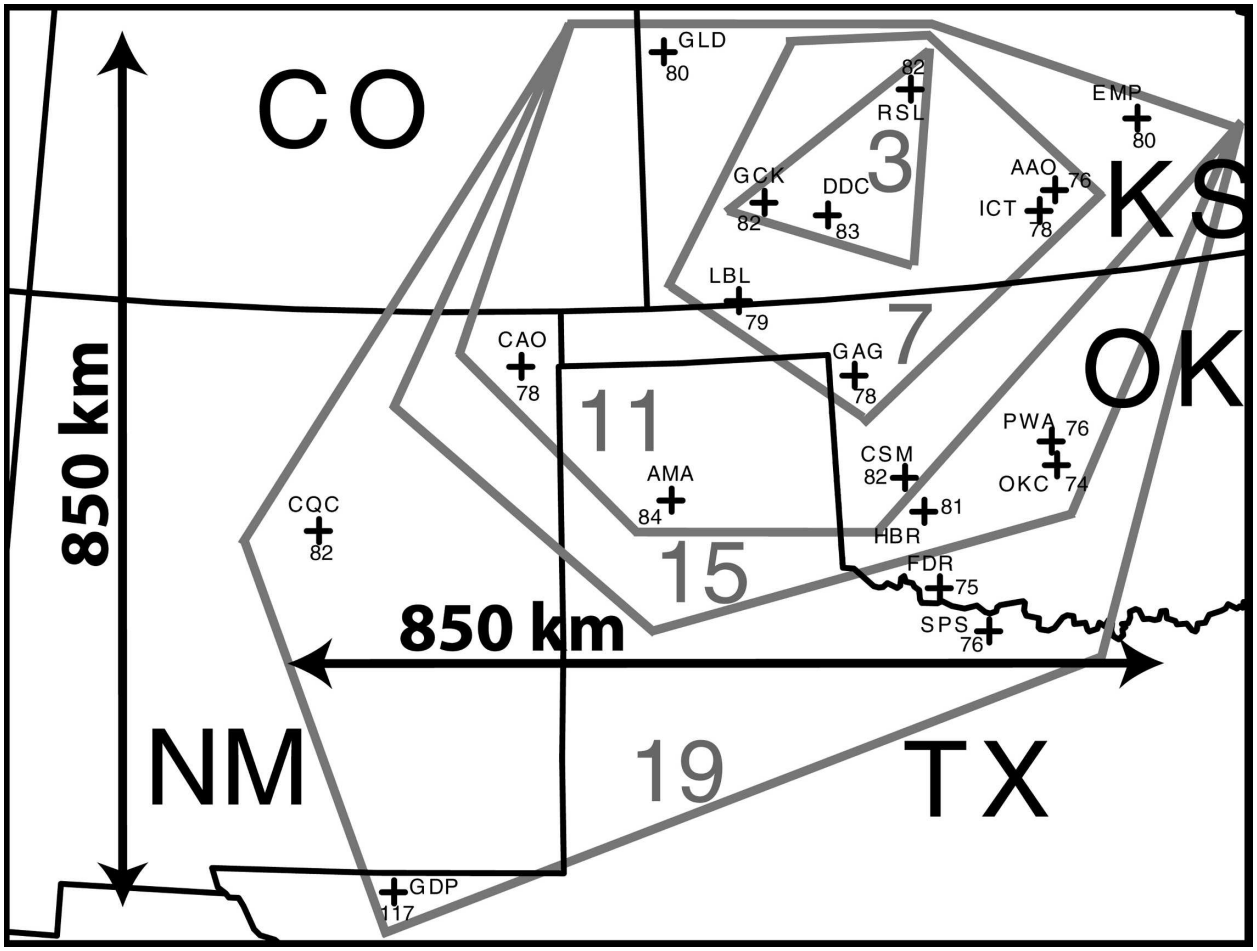

FIG. 2. Locations of the 19 sites used in arrays. Sites included in the 3-, 7-, 11-, 15-, and 19-site array configuration based on geography only are grouped within gray lines; also shown are annual average wind speeds (10^{-1} m s^{-1}) at each site.

sible combinations of sites that can be included is large (Table 2). For example, there are 50 388 possible combinations of seven sites among the 19 of interest. The "base case" for this study is based solely on geographical proximity, and it is described in Table 1. Unless otherwise stated, all possible combinations of sites for each array size are evaluated in the rest of this study.

b. Results

The analysis indicated that the reliability of interconnected wind systems increased with the number of farms. Reliability in this context is defined in terms of a "generation duration curve," also known as a "duration curve" (Nørgård et al. 2004; Holttinen and Hirvonen 2005), which is analogous to the load duration curve used for electricity demand. All hours in a year (i.e., $365 \times 24 = 8760$) are rearranged based on decreasing wind power magnitude, and the corresponding power is plotted as a decreasing curve. The generation curve can also be interpreted as a "reversed" cumulative probability distribution, in which each point on the x axis represents the probability (in terms of number of hours in a year) of wind power production greater or equal to the corresponding y value on the curve. The adjective reversed was used because a traditional cumulative probability distribution is monotonically increasing, and it shows the probability of the variable being lower or equal to the value on the curve.

Figure 3 shows generation duration curves for the 1-, 7-, and 19-site base-case arrays. For the figure, all hours in a year, less 2% of randomly selected hours where wind turbines were assumed to be down because of unplanned maintenance, were rearranged based on decreasing wind power magnitude per hour. For simplicity, each site is considered to have a single GE 1500-kW turbine (General Electric 2004), and each curve shows the wind power output per turbine, averaged over all sites in the array. For the seven-site array, for example, each point shows the total power produced by the array divided by the number of sites (seven at most) with

TABLE 1. List of selected sites and their properties (ID means identifier).

ID	Name	State	Yearly V80	Power class	No. of sites in array(s)
DDC	Dodge City	KS	8.3	5	1, 3, 7, 11, 15, 19
GCK	Garden City	KS	8.1	5	3, 7, 11, 15, 19
RSL	Russell	KS	8.2	5	3, 7, 11, 15, 19
LBL	Liberal	KS	7.9	4	7, 11, 15, 19
GAG	Gage	OK	7.8	4	7, 11, 15, 19
ICT	Wichita	KS	7.8	4	7, 11, 15, 19
AAO	Wichita–Col. Jabar	KS	7.6	4	7, 11, 15, 19
GLD	Goodland Renner	KS	8.0	4	11, 15, 19
EMP	Emporia	KS	8.0	4	11, 15, 19
CAO	Clayton	NM	7.8	4	11, 15, 19
CSM	Clinton	OK	8.2	5	11, 15, 19
AMA	Amarillo	TX	8.4	5	15, 19
OKC	Oklahoma City	OK	7.4	3	15, 19
HBR	Hobart	OK	8.1	5	15, 19
PWA	Oklahoma City	OK	7.6	4	15, 19
FDR	Frederick	OK	7.5	3	19
SPS	Wichita Falls	TX	7.6	4	19
CQC	Clines Corner	NM	8.2	5	19
GDP	Pine Springs	TX	11.7	7	19

available data at that hour. Because of missing values, none of the three curves had valid data for all 8760 h, but each curve had a different number of valid hours. As such, for example, the 92% probability line corresponds to a slightly different number of hours for each array size.

"Firm capacity" is the fraction of installed wind capacity that is online at the same probability as that of a coal-fired power plant. On average, coal plants are free from unscheduled or scheduled maintenance for 79%–92% of the year, averaging 87.5% in the United States from 2000 to 2004 (Giebel 2000; North American Electric Reliability Council 2005). Figure 3 shows that, while the guaranteed power generated by a single wind farm for 92% of the hours of the year was 0 kW, the power guaranteed by 7 and 19 interconnected farms was 60 and 171 kW, giving firm capacities of 0.04 and 0.11, respectively. Furthermore, 19 interconnected wind farms guaranteed 222 kW of power (firm capacity of 0.15) for 87.5% of the year, the same percent of the year that an average coal plant in the United States guarantees power. Last, 19 farms guaranteed 312 kW of power for 79% of the year, 4 times the guaranteed power generated by one farm for 79% of the year.

Capacity factor is the fraction of the rated power (or maximum capacity) actually produced in a year. The capacity factor of the 19-site array was ~0.45, corre-

TABLE 2. Statistics of interconnected wind power from aggregate arrays as a function of the number of sites included. Values obtained with the absolute value of A in Eq. (7) are in parentheses.

No. of sites	1	3	7	11	15	19
No. of combinations analyzed	19	969	50 388	75 582	3876	1
Array-average wind speed ($m\,s^{-1}$)	8.25 (8.24)	8.12 (8.12)	8.12 (8.11)	8.12 (8.11)	8.12 (8.11)	8.12 (8.11)
Std dev of array-average wind speed ($m\,s^{-1}$)	4.36 (4.34)	3.47 (3.46)	3.05 (3.05)	2.93 (2.93)	2.87 (2.87)	2.84 (2.84)
Array-average wind power (kW)	680.69 (680.87)	665.39 (665.33)	665.11 (665.01)	665.16 (665.06)	665.14 (665.03)	665.13 (665.02)
Std dev of array-average wind power (kW)	569.85 (569.20)	448.47 (448.31)	394.07 (394.21)	378.01 (378.22)	370.35 (370.59)	365.85 (366.12)
Total wind energy (MWh)	5189 (5191)	15 568 (15 573)	36 326 (36 336)	57 084 (57 099)	77 842 (77 862)	98 600 (98 625)
Mean capacity factor (%)	45.38 (45.39)	45.32 (45.33)	45.30 (45.31)	45.29 (45.31)	45.29 (45.30)	45.29 (45.30)
Firm capacity, base case (at 87.5% and 79% probability)	0.00	0.04	0.06	0.10	0.11	0.15
	0.05	0.09	0.12	0.16	0.14	0.21
Reserve requirements (MWh) per site, test case only	835	641	513	452	438	403

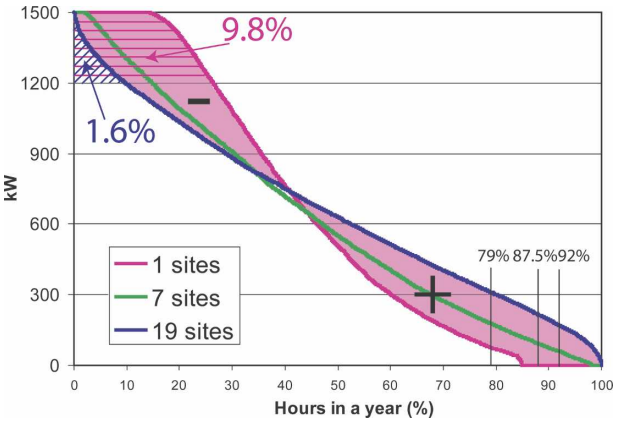

FIG. 3. Generation duration curves for base-case array configurations: single-, 7-, and 19-site arrays. Each point on the *x* axis represents the percent of hours in a year that wind power production is greater than or equal to the corresponding power (*y* axis) on the curve. The area below the generation curve represents the total energy (kWh) produced in a year by the array. Shaded areas are described in the text. The thatched areas are the energy lost (9.8% and 1.6%) if the size of transmission lines is reduced from 1500 to 1200 kW for the 1- and 19-site arrays, respectively.

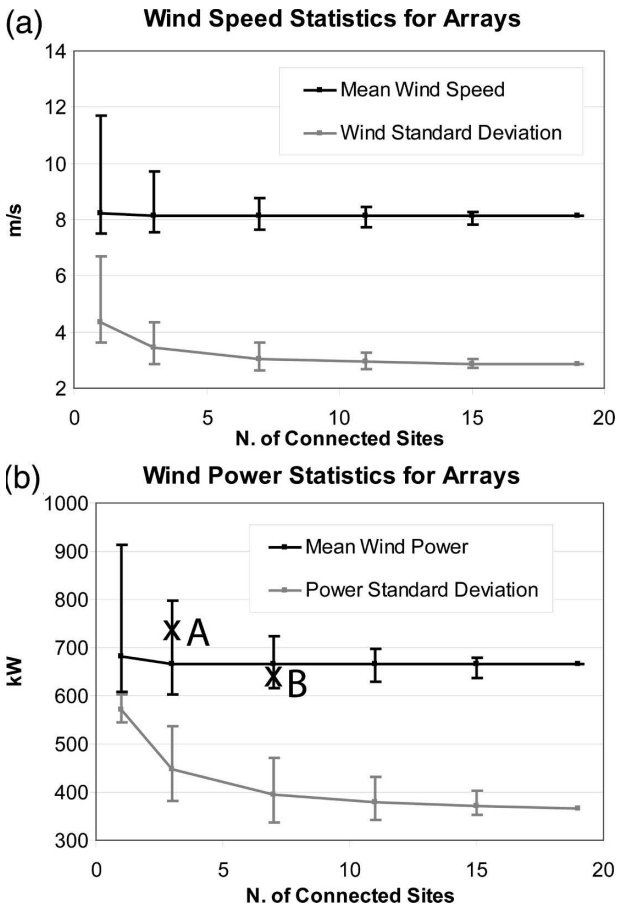

FIG. 4. (a) Wind speed and (b) wind power statistics for interconnected arrays as a function of number of connected sites. The bars indicate the range of values obtained from all possible combinations of the given number of connected sites.

sponding to a yearly power of ~670 kW (Table 2). The resulting ratio of the guaranteed power produced at 79% reliability to the yearly power produced by the 19-site array was 312 kW/670 kW or ~47%. Thus, the firm power produced for 79% of the year by a 19-site array was almost half of the actual power produced in the year or 21% of the maximum possible power produced. At the 12.5% outage rate for coal, the guaranteed power produced was 222 kW/670 kW or ~33% of the yearly power produced.

Although the 1-site array had more hours of power production at the rated power than did an average of the 19-site array (149 vs 9), the 19-site array had fewer hours with no power (5 vs 170) and more overall hours with low power production than did the 1-site array (Fig. 3). Similar findings were shown by Holttinen and Hirvonen (2005) for a single turbine, an array covering western Denmark, and a hypothetical array covering four northern countries in Europe. The area below the generation curve represents the total energy (kWh) produced in a year by the array. For ~38% of the hours, less energy was produced, averaged over 19 farms, than for an individual farm (deficit denoted by the "−" mark). However, this lower average production was made up for by higher average production for the 19 sites over the remaining 62% of the hours (surplus denoted by the "+" mark).

Given an array of size *K*, there is a large number of possible combinations of *K* sites among 19 (Table 2). All possible combinations were analyzed in this study. To facilitate the comparison, however, only the average of all combinations for each array size and for each parameter are shown in Table 2. For example, the total energy produced in a year by all possible seven-site arrays varied between 32 529 (worst combination) and 39 478 MWh (best combination); the average from all 50 388 combinations was 36 326 MWh, the value shown in Table 2. Similarly, the figures show the averages of all combinations as a function of the number of interconnected sites, and the range of values from all combinations is shown by the bars.

All parameters that depended linearly on the sites values, such as array-average wind speed, power, total energy, and capacity factor, were unchanged whether or not the sites were interconnected, as expected (Table 2). Nonlinear parameters, such as wind speed standard deviation, firm capacity, and reserve requirements, showed large improvements. For example, the standard deviations of array-average wind speed and power monotonically decreased (Table 2; Fig. 4). Also, the

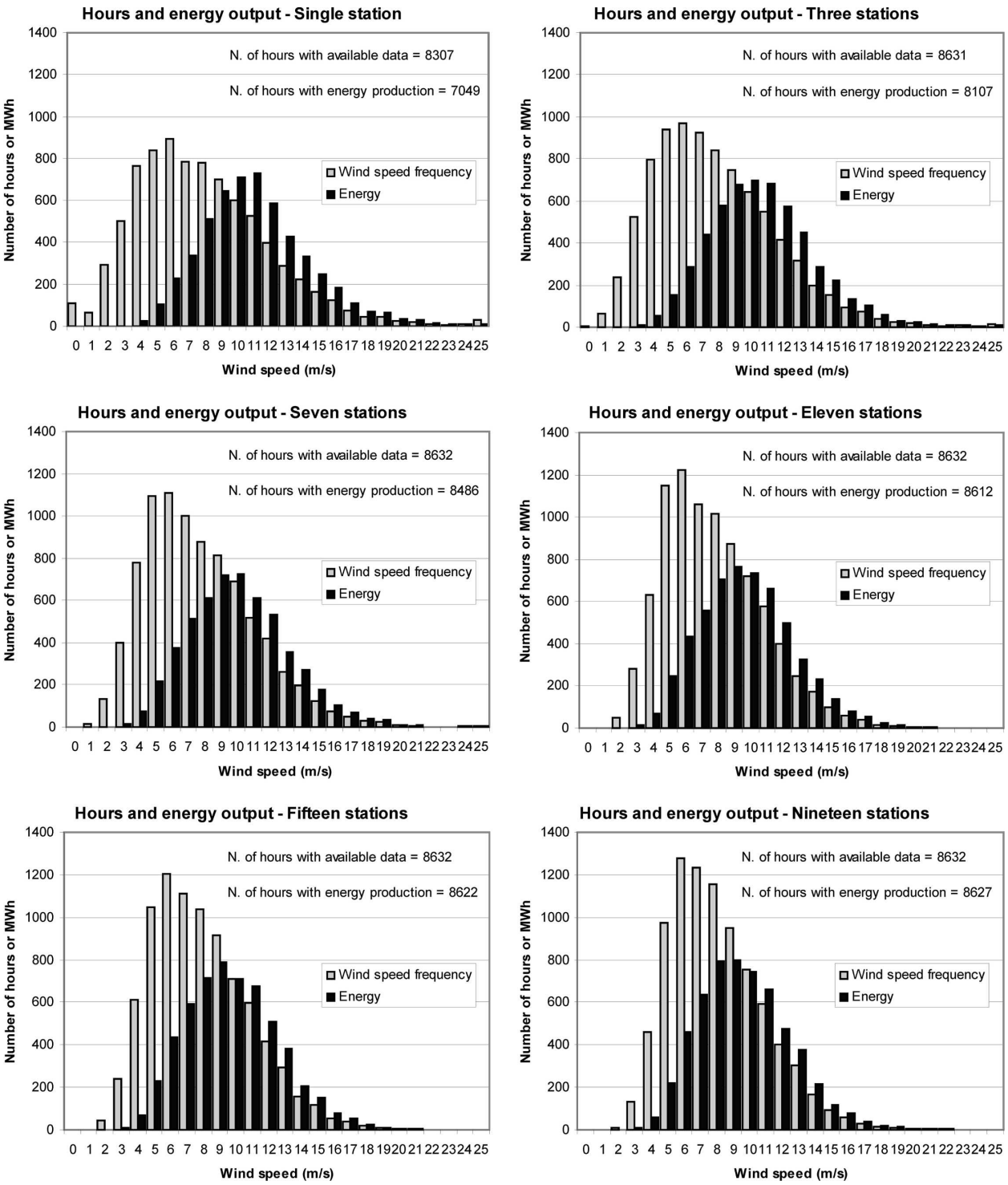

FIG. 5. Number of hours and energy output (kWh) at given wind speeds (m s^{-1}) for all hours of 2000 averaged over (a) 1, (b) 3, (c) 7, (d) 11, (e) 15, and (f) 19 stations.

frequency distribution of wind speed shifted to the right and became more symmetric as the number of stations included in the network increased (Fig. 5). This is consistent with previous findings by Archer and Jacobson (2003) and indicates that the array wind speed distribution is closer to Gaussian than it is to Rayleigh. As such, the more sites that are interconnected, the more the array resembles a single farm with steady winds.

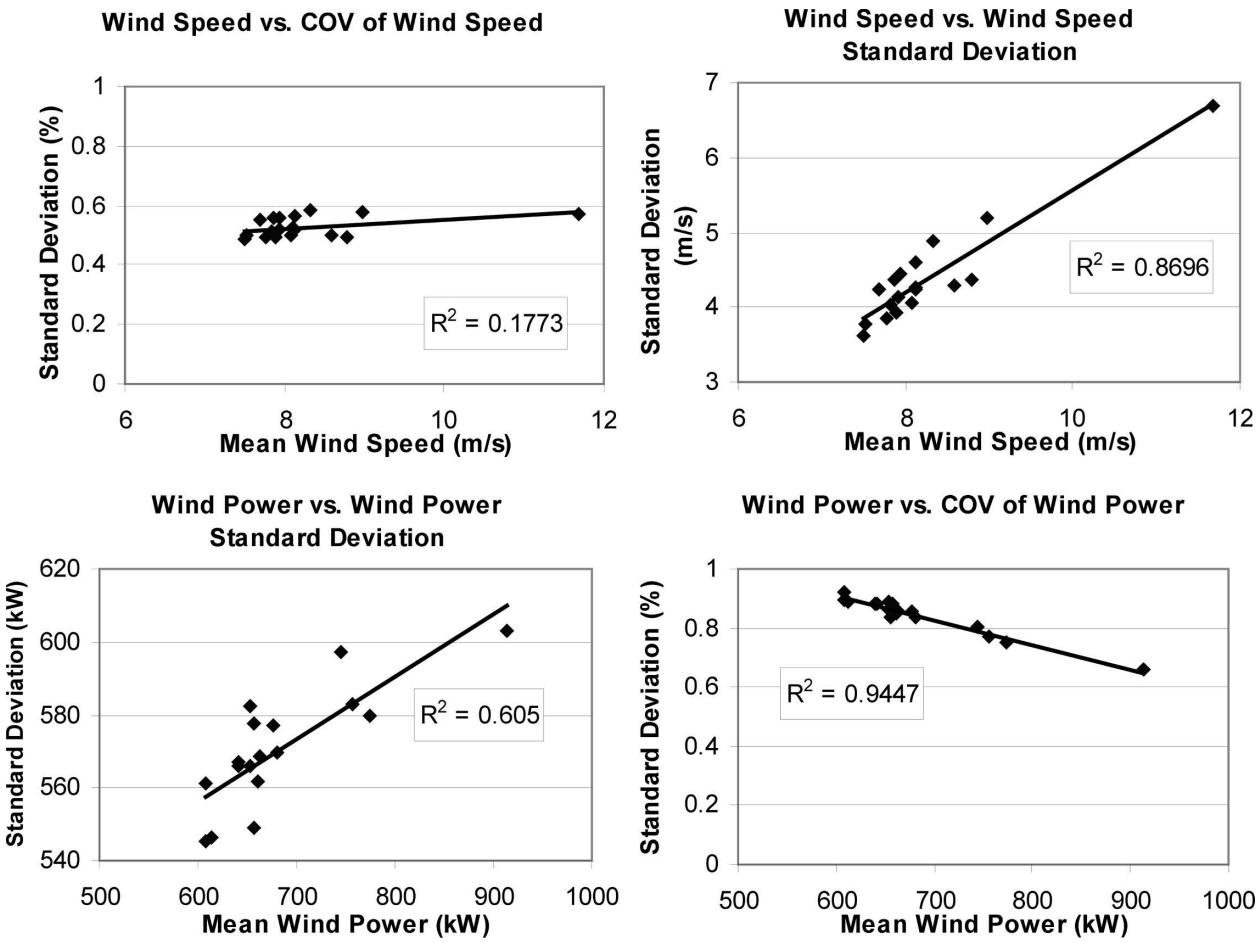

FIG. 6. Standard deviations and coefficients of variation of wind speed and wind power at the 19 sites selected.

Second, it appears that marginal benefits decrease with an increase in the number of farms. In other words, even though all nonlinear parameters improved as the number of farms went up, the incremental benefit of adding new stations kept decreasing. This is consistent with both common sense and Kahn (1979). Figure 4 shows that wind speed and wind power standard deviations decreased less than linearly with an increasing number of sites. Note, however, that no saturation of the benefits was found, or, in other words, an improvement was obtained, even if small, for every addition to the array size.

Third, the optimal configuration was not necessarily the one with the highest number of sites. Figure 4b shows that some combinations of seven sites (e.g., point A in the figure) produced higher array-average wind power than some other combinations of 11 sites (e.g., point B). The same applied to all other statistics. However, so long as more sites were added to a given array in such a way that the area covered became increasingly larger (as in the base case), statistical correlation among the sites decreased and so did standard deviations (Table 2 and Fig. 4), thus improving array reliability and performance. Note that array-average wind speed and power may become lower for increasingly larger areas if sites in lower wind power class are added to the initial pool.

Is there a trade-off between wind speed and intermittency? Simonsen and Stevens (2004) found that, as single-site wind speed increases, so does the ratio between single-site wind speed standard deviation and standard deviation of array-average wind speed (linearly). An incorrect interpretation of this finding would be that, as average wind speed increases, so does intermittency. While it is true that wind power (speed) standard deviation increases as wind power (speed) increases (Figs. 6a,b), this is not indicative of increased intermittency. One should not look at standard deviation per se, but at standard deviation and mean wind speed together to evaluate intermittency. A better parameter to look at is the ratio of standard deviation over the mean. This ratio, known as "coefficient of

variation" (COV), behaved differently for wind speed versus wind power. For wind speed (Fig. 6c), the COV was approximately independent of wind speed, which suggests that wind speed standard deviation is approximately a constant percent of mean wind speed; consequently, intermittency is not increased at higher average wind speed sites but it is almost constant. COV of wind power, on the other hand, linearly decreased for increasing array-average wind power (Fig. 6d), with a high correlation coefficient (−0.97). This also suggests that wind power intermittency is actually reduced at sites belonging to higher wind power classes, and thus it is more advantageous to select sites with high year-mean wind speed, a finding consistent with Archer and Jacobson (2003). This is due to the fact that, since wind power is constant for wind speeds greater than the rated wind speed, less variation is introduced at high wind speeds.

Further details can be found by looking at cumulative frequency distributions of wind array-average wind speed (Fig. 7a). What is desirable is a curve that has small frequencies at low wind speeds and that rapidly reaches its maximum of one. The transition from one to three sites brings little improvement, whereas a large benefit at both low and high wind speeds is reached with the seven-site configuration. The addition of 3, 8, and 11 sites (to a total of 11, 15, and 19) does not improve substantially the array performance at high wind speeds, but it improves that at low speeds, especially with the 19-site array.

Which sites should one select, given the large number of possible combinations? It depends on the objective: minimization of costs, minimization of load swings during peak hours, maximum reliability overall, and maximum average wind power are among them. Note that geographic proximity was the only factor for the base case. Milligan and Artig (1998) used a production cost/reliability model to compare several indicators to find the most reliable site configuration (among six Minnesota sites), including lowest loss-of-load expectation (LOLE) and lowest expected energy not served (ENS), in both a deterministic and a "fuzzy logic" approach. They found that the fuzzy method applied to ENS was the most robust measure of system reliability and that the optimal configuration was one with only four out of six sites. Milligan and Artig (1999) further applied this technique to a multiyear dataset and found that interannual variability had an impact on the selection of the best sites. In general, it is preferable to connect sites that can provide more reliability, even with lower average wind speed, than vice versa. Figure 5 shows that, as the number of connected sites increased, the behavior of the array resembled more and more that of a site

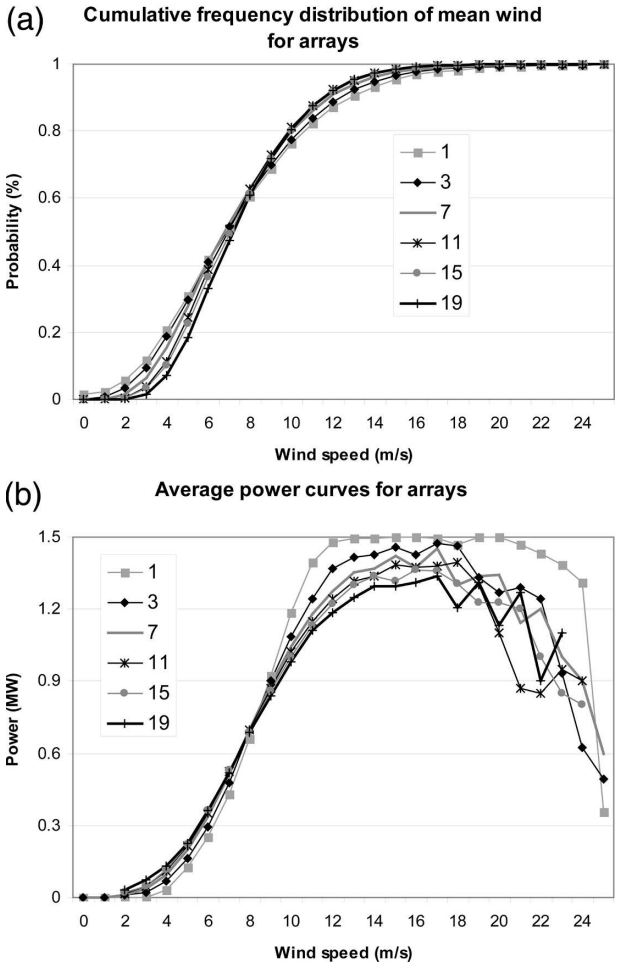

FIG. 7. (a) Cumulative frequency distribution and (b) wind power curve (MW) as a function of wind speed (m s^{-1}), obtained after an array average.

with steady but not necessarily strong wind speed. Large arrays did not provide more power at high speeds, but rather more power at low speeds, when compared with smaller arrays (Fig. 7b). Note how the array-averaged power curve did not reach asymptotically the rated power of the individual turbine. In fact, since no power can be produced when the wind is too strong (i.e., above 25 m s^{-1}), fewer sites contributed to the total array power when the array-average wind speed was large (i.e., above $V_{\text{rated}} = 12$ m s^{-1}).

As wind speed standard deviation decreases for larger arrays, reserve requirements are reduced when compared with each individual farm and with the sum of all farms if they were not connected. The latter configuration will be referred to as "linear sum." An exact expression for the reserve requirements would be hard to obtain, as it is a function of the electricity bidding prices on the market, the forecast load and winds, and

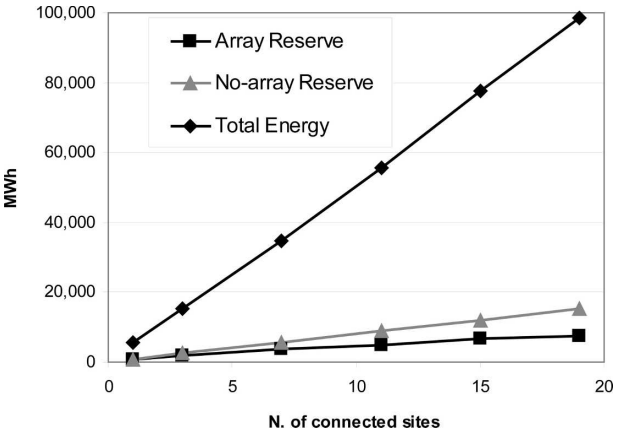

FIG. 8. Reserve requirements in a year (MWh) for the base-array and for the no-array cases (sites if they were not interconnected). Total energy (MWh) produced by the array in a year is also shown.

the exact type of backup system. A simple assumption is the persistency model, that is, at each hour h, the base array commits to producing the same power supplied the previous hour $h - 1$. Other energy sources provide peaking capacity during the year. The advantage of its relatively simple formulation is that reserve requirements of interconnected arrays can be calculated easily.

Results are summarized in Fig. 8. For the single-site configuration only, reserve requirements coincided for the array and the linear-sum cases (by definition). As more sites were interconnected, the array had substantially lower reserve requirements than the linear sum. For example, for the three-site configuration, average reserve energy per site decreased from 2103 to 1713 MWh a year (i.e., 19% reduction) when compared with the single-site case. The greatest benefit was for the largest array, with an ~60% decrease in reserve requirements when compared with the linear sum of 19 sites (Table 2) and an ~47% decrease when compared with the single-site case. As array size increased, reserve requirements represented a decreasing fraction of the total energy produced (Fig. 8). For the three-site configuration, 5138 MWh were needed as reserve in a year, corresponding to ~33% of the total energy production (15 438 MWh per year); for the 11-site configuration, this fraction was slightly lower than 25% and for the 19-site array it was ~21%.

A final benefit of interconnecting wind farms is that it can allow long-distance transmission from a common point, where several farms are connected, to a high-load area to be reduced with little loss of transmitted power. Suppose we want to bring power from N independent farms (each with a maximum capacity of, say, 1500 kW), from the Midwest to California. Each farm would need a short transmission line of 1500 kW brought to a common point in the Midwest. Between the common point and California, the size of the transmission line would normally need to be $N \times 1500$ kW. However, because geographically disperse farms cause slow winds in some locations to cancel fast winds in others, the long-distance transmission line could be reduced by 20% (to $N \times 1200$ kW) with only a small loss (2% with $N = 19$) in overall delivered power (Fig. 3). With only one farm, a 20% reduction in long-distance transmission would decrease delivered power by 9.8%. Thus, the more wind farms connected to the common point in the Midwest, the greater the reduction in long-distance transmission capacity possible with little loss in delivered power. Because of the high cost of long-distance transmission, a 20% reduction in transmission capacity with little delivered power loss would reduce the cost of wind energy.

3. Validation

The LS method was evaluated against observed data from the Kennedy Space Center (KSC) tower network (Fig. 9), described in detail in Archer and Jacobson (2005). The wind speed data used so far were retrieved at a reference height $H^{\mathrm{REF}} = 10$ m and were extrapolated to a hub height $H^{\mathrm{HUB}} = 80$ m, thus the notation V10 and V80 for the reference and the hub height wind speeds. However, the LS method can be applied to any paired reference and hub heights. Furthermore, the KSC data were retrieved at variable heights (Table 3). Therefore, the notation V^{REF} and V^{HUB} will be used in the rest of this section.

The validation will focus on two aspects of the LS method. The first one is the potential error introduced when daily averages of V^{REF} are used in combination with 2-times-per-day sounding profiles, as opposed to more frequent and simultaneous surface and sounding profiles. This step is relevant for optimal wind farm siting when only daily averages of V^{REF} are available. In this rather common case, it is important to know whether (and how much) LS results could be biased. The second aspect is the formulation of the hourly evolution of V^{HUB} given observed hourly V^{REF}. Both aspects will be examined in the next two sections.

a. Error in using daily averages

As discussed in Archer and Jacobson (2005), the LS method should be applied with simultaneous sounding and surface data. In other words, for each given hour, the LS parameters should be determined from the soundings and then applied to the value of V^{REF} at the

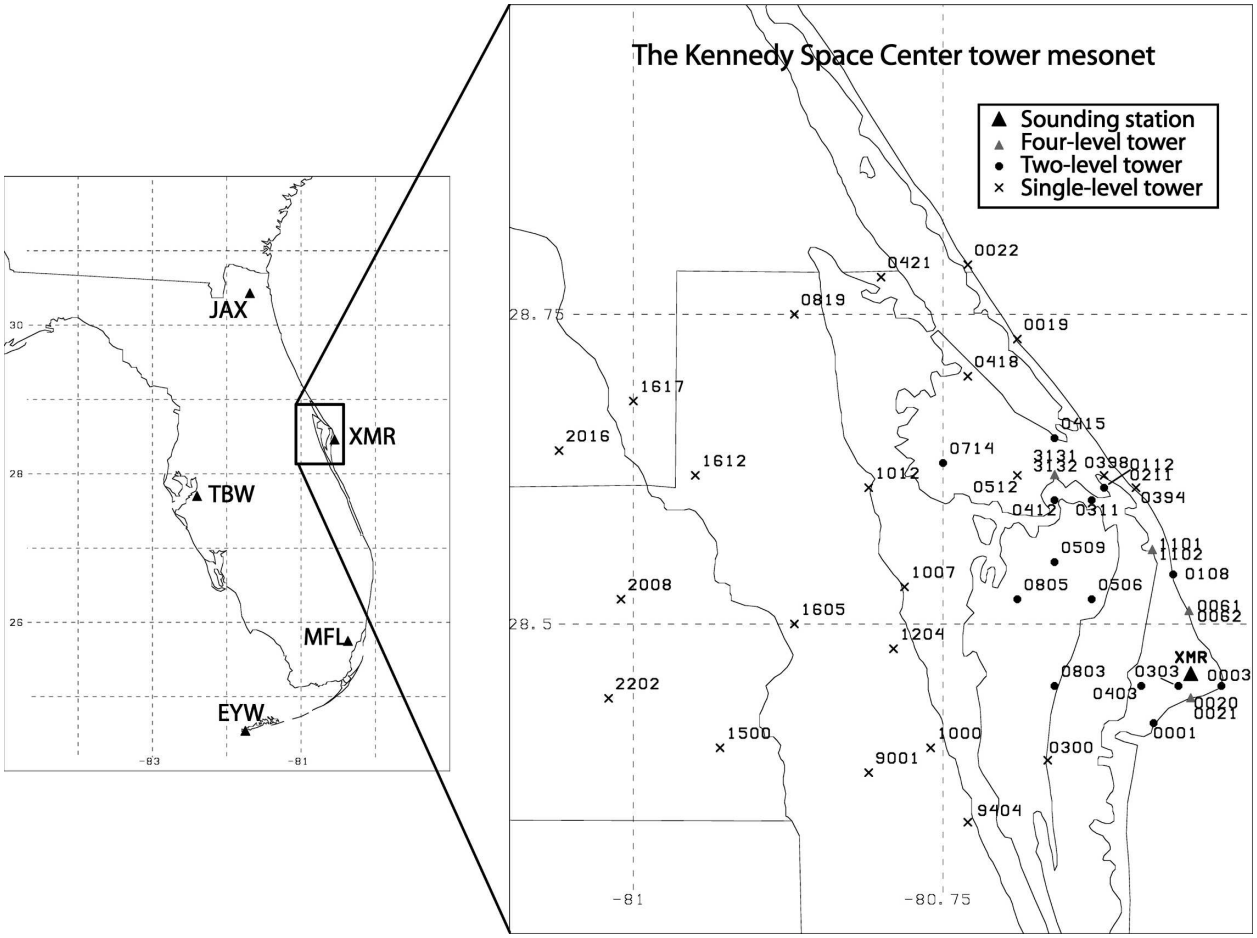

FIG. 9. Location of sounding stations and towers near the KSC.

surface station, valid at the same hour as the soundings. The daily average of V^{HUB} at the surface station should then be calculated from hourly values as follows:

$$\overline{V_H^{\mathrm{HUB}}} = \frac{1}{24} \times \left\{ \sum_{h=1}^{24} \frac{1}{\sum_{k=1}^{K} \frac{1}{R_k^2}} \times \left[\sum_{k=1}^{K} \frac{1}{R_k^2} L_{h,k}(V_h^{\mathrm{REF}}) \right] \right\}, \tag{3}$$

where $L_{h,k}$ is the LS function [as in Archer and Jacobson (2005)] at sounding station k for hour h, V_h^{REF} is the hourly average of V^{REF} at the surface station, and $\overline{V_H^{\mathrm{HUB}}}$ is the daily average of $\mathrm{V}^{\mathrm{HUB}}$ at the surface station as determined from hourly values.

However, neither sounding nor surface data are available on an hourly basis for all locations. Daily averages of wind speeds at the surface stations and 2-times-per-day sounding profiles are often the only available data. For the typical case of two sounding profiles (at 0000 and 1200 UTC), the estimate of the daily average wind speed at hub height based on daily average reference height wind speed $\overline{V_D^{\mathrm{REF}}}$ was therefore

$$\overline{V_D^{\mathrm{HUB}}} = \frac{1}{\sum_{k=1}^{K} \frac{1}{R_k^2}} \times \left[\sum_{k=1}^{K} \frac{1}{R_k^2} \times \frac{L_{00,k}(\overline{V_D^{\mathrm{REF}}}) + L_{12,k}(\overline{V_D^{\mathrm{REF}}})}{2} \right], \tag{4}$$

where $L_{00,k}$ and $L_{12,k}$ are calculated at 0000 and 1200 UTC, respectively, from each sounding station k.

Archer and Jacobson (2005) used data from the KSC network to conclude that Eq. (4) was an acceptable (and conservative) approximation for Eq. (3). In this study, the same dataset is used to evaluate further the extent of the error introduced in Eq. (4) and the dependence of such error on the time zone of the stations of interest.

TABLE 3. List of the Kennedy Space Center towers and levels. The reference and the hub heights are indicated with "ref" and "hub," respectively.

Tower ID	No. of levels	Levels (m)						
0020	(All)	4	16 (ref)	27	44 (hub)	62		
	($N = 3$)		16 (ref)	27	44 (hub)	62		
0021	(All)	4	16 (ref)	27	44 (hub)	62		
	($N = 3$)		16 (ref)	27	44 (hub)	62		
0061		4 (ref)	16	49 (hub)	62			
0062		4 (ref)	16	49 (hub)	62			
1101		4 (ref)	16	49 (hub)	62			
1102		4 (ref)	16	49 (hub)	62			
3131	(All)	4	16 (ref)	49 (hub)	62	90	120	150
	($N = 3$)		16 (ref)	49 (hub)	62			150
3132	(All)	4	16 (ref)	49 (hub)	62	90	120	150
	($N = 3$)		16 (ref)	49 (hub)	62			150
0001		4 (ref)	16 (hub)					
0108		4 (ref)	16 (hub)					
0112		4 (ref)	16 (hub)					
0211		4 (ref)	16 (hub)					
0303		4 (ref)	16 (hub)					
0311		4 (ref)	16 (hub)					
0403		4 (ref)	16 (hub)					
0412		4 (ref)	16 (hub)					
0415		4 (ref)	16 (hub)					
0506		4 (ref)	16 (hub)					
0509		4 (ref)	16 (hub)					
0714		4 (ref)	16 (hub)					
0803		4 (ref)	16 (hub)					
0805		4 (ref)	16 (hub)					

Following Archer and Jacobson (2005), the KSC towers are divided into two categories: four-level towers, with wind speed sensors at four or more heights, and two-level towers, with sensors at only two heights. The eight four-level towers (Table 3) can be used as surrogates for sounding stations because LS parameters can be determined only if wind data are available at least for three heights. They will be referred to as "surrogate soundings." At these towers, H^{REF} and H^{HUB} were chosen so as to mimic the typical sounding profiles, for which H^{REF} is the lowest available height and two heights are typically available above H^{HUB}. At the same time, it was preferable to have H^{HUB} as close as possible at all eight towers to make easier the comparison among them. Because of this requirement, different towers have different pairs of H^{REF}–H^{HUB}, but all have $H^{\mathrm{HUB}} \sim 50$ m. Also, H^{REF} was preferably ~ 10 m. For an evaluation of the LS method at these eight surrogate sounding towers, refer to Archer and Jacobson (2005, their Table 7), which showed that the average error was approximately −3%. The 14 two-level towers can be treated as surface stations ("surrogate surface"). At these surrogate surface towers, the average error was −19.8% (Archer and Jacobson 2005, their Table 8). The following analysis will focus on these 14 towers, for all of which $H^{\mathrm{REF}} = 4$ m and $H^{\mathrm{HUB}} = 16$ m.

Given the time zone of the KSC network (i.e., −5 from UTC), the 0000 and 1200 UTC hours correspond to 1900 and 0700 LST, respectively. LS parameters were thus calculated at 0700 and 1900 LST from the surrogate soundings and used at the surrogate surface stations. Results are summarized in Table 4. Note that the values in Table 4 differ from those in Table 8 of Archer and Jacobson (2005) because the latter were obtained from five real sounding profiles retrieved in Florida, and not from the surrogate sounding towers, as done here.

Equation (3) appears to be a good estimator of V^{HUB}, as the average observed V^{HUB} was 3.34 m s^{-1} and the average calculated V^{HUB} from hourly values was 3.04 m s^{-1}. For each individual station, $\overline{V_H^{\mathrm{HUB}}}$ was conservative at all stations except for towers 0112, 0211, 0403, and 0506, with the worst overestimate being 20.2% at tower 0403. Note that towers 0112 and 0211 are collocated.

By using daily averages in combination with 2-times-per-day LS parameters determined from surrogate soundings (i.e., $\overline{V_D^{\mathrm{HUB}}}$) with Eq. (4), the accuracy of the result depends on the time zone of the station, or, in other words, on which 12-h-apart pairs of hours are used. For example, by using the 0700–1900 LST pair at tower 0311, results obtained with Eq. (4) (4.05 m s^{-1})

TABLE 4. Values of observed and calculated LS wind speeds at KSC two-level towers. Calculated values were obtained by either simultaneous V_{ref} and sounding parameters (hourly) or by using the daily average of V_{ref} with 12-h-apart sounding parameters. In boldface are the average observed wind speeds and those calculated from hourly profiles; also in boldface are the average wind speeds calculated from 2-times-per-day profiles for the time zones of the United States.

			Sounding times (LST)										
Tower	Obs	Hourly	0000–1200	0100–1300	0200–1400	0300–1500	0400–1600	0500–1700	0600–1800	0700–1900	0800–2000	0900–2100	1000–2200	1100–2300
0001	3.70	2.24	2.23	2.24	2.26	2.29	2.32	2.39	2.44	2.40	2.29	2.24	2.22	2.22
0108	3.51	2.60	2.50	2.49	2.52	2.54	2.56	2.61	2.67	2.64	2.57	2.54	2.51	2.51
0112	3.65	3.69	3.64	3.63	3.66	3.69	3.71	3.82	3.99	3.91	3.79	3.73	3.68	3.68
0211	4.24	4.34	4.24	4.21	4.35	4.43	4.48	4.54	4.66	4.65	4.42	4.17	4.15	4.23
0303	2.97	2.31	2.33	2.34	2.36	2.41	2.44	2.51	2.59	2.54	2.43	2.36	2.32	2.33
0311	3.96	3.86	3.79	3.80	3.80	3.84	3.88	3.97	4.12	4.05	3.92	3.87	3.79	3.82
0403	3.68	4.42	4.32	4.34	4.38	4.45	4.49	4.62	4.73	4.63	4.46	4.35	4.30	4.30
0412	3.20	2.72	2.76	2.76	2.76	2.80	2.83	2.91	3.03	2.94	2.85	2.77	2.75	2.77
0415	2.98	2.60	2.64	2.63	2.60	2.66	2.68	2.77	2.91	2.85	2.74	2.67	2.63	2.64
0506	3.34	3.72	3.62	3.62	3.64	3.64	3.67	3.70	3.72	3.75	3.72	3.70	3.62	3.64
0509	3.08	2.86	2.84	2.84	2.82	2.84	2.86	2.91	3.01	2.96	2.93	2.87	2.84	2.84
0714	3.26	2.40	2.41	2.40	2.38	2.42	2.44	2.51	2.60	2.53	2.47	2.44	2.39	2.41
0803	2.43	2.29	2.27	2.27	2.30	2.33	2.35	2.42	2.48	2.45	2.35	2.28	2.26	2.27
0805	2.72	2.51	2.51	2.50	2.52	2.53	2.55	2.59	2.66	2.60	2.54	2.54	2.50	2.51
Avg	**3.34**	**3.04**	3.01	3.01	3.03	3.06	3.09	**3.16**	**3.26**	**3.21**	3.11	3.04	3.00	3.01

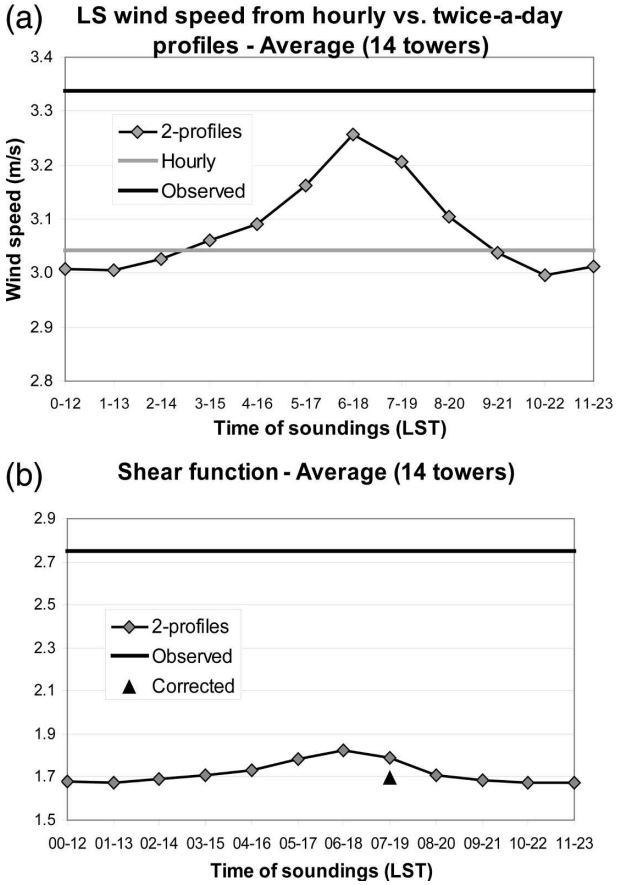

FIG. 10. (a) Observed winds, calculated from hourly V_{ref}, and calculated from daily averages of V_{ref} with 2-times-per-day soundings values of LS wind speed, averaged over all two-level towers of the KSC network. (b) Values of the shear function ρ averaged over all hours and all KSC two-level towers obtained with all 12-h-apart pairs of sounding times. The value obtained with correction factors at 0700–1900 LST (corresponding to 0000 and 1200 UTC in Florida) is shown with a rhomboidal mark. Reproduced from Archer and Jacobson (2006).

are slightly larger than those obtained with Eq. (3) (3.86 m s^{-1}). The same applies to the six 12-h-apart pairs between 0300–1500 and 0800–2000 LST. For all other pairs, a small underestimate is instead introduced by using daily averages. Figure 10a shows that, on average, pairs between 0500–1700 and 0700–1900 LST, that is, the three easternmost time zones of the United States, generate estimates of V^{HUB} that are larger than those generated with simultaneous sounding and surface hourly values. However, such estimates are lower than observations by −2.4% on average, with −35.3% (tower 0001 at 0500–1700 LST) and +28.7% (tower 0403 at 0600–1800 LST) as extremes.

In summary, the application of the LS method to simultaneous surrogate sounding and surrogate surface hourly values appears to be generally accurate and con-

servative. By using daily averages at surrogate surface stations in combination with 2-times-per-day LS parameters derived from surrogate soundings, results differ slightly depending on the time zone. If the LS parameters are obtained in the late afternoon and early morning (i.e., 0500–1700, 0600–1800, and 0700–1900 LST), V^{HUB} estimates are larger than those obtained from hourly values, but still smaller than observed values on average. As such, the LS method appears to be acceptable and conservative even when used with daily averages of V^{REF}.

b. *Error in using the ρ function (with and without correction factors)*

From Archer and Jacobson (2003), the variation with time h of the ratio between V^{HUB} and V^{REF}, also known as the shear function $\rho(h)$, can be represented as a sinusoidal as follows:

$$\rho(h) = \bar{\rho} + A \sin\left[\frac{\pi}{12}(h - \delta)\right], \tag{5}$$

where A is the curve amplitude, δ is the time shift necessary for the sine curve to have a minimum at 1300 LT (-5), and $\bar{\rho}$ is the daily mean of ρ. The hourly values of V^{HUB} can then be obtained by multiplying hourly values of V^{REF} by $\rho(h)$. If only the values of ρ at 0000 and 1200 UTC are known (i.e., ρ_{00} and ρ_{12}), then the two unknown parameters $\bar{\rho}$ and A can be estimated as

$$\bar{\rho} = \alpha \frac{\rho_{12} + \rho_{00}}{2} \quad \text{and} \tag{6}$$

$$A = \beta \frac{\rho_{12} - \rho_{00}}{2}, \tag{7}$$

where α and β are factors depending on the time zone. Note that amplitude A in Eq. (7) is allowed to become negative (when $\rho_{00} > \rho_{12}$), to capture the real variability of the shear function. However, Eq. (7) was originally derived for the central U.S. time zones, for which ρ has a minimum around 0000 UTC. In Florida, ρ at 0000–1200 UTC is near zero, which could cause spurious sign switches in the amplitude value. Thus, in this section only, the absolute value was used in Eq. (7). This choice was also introduced to avoid sign dependency on the time zone. The absolute-value formulation was generally conservative at most of the stations tested (as discussed later), and it is consistent with findings by Lazarus and Bewley (2005).

After combining Eq. (5) with Eqs. (6) and (7), ρ_h can be expressed as

$$\rho_h = \alpha \frac{\rho_{12} + \rho_{00}}{2} + \beta \frac{\rho_{12} - \rho_{00}}{2} \sin\left[\frac{\pi}{12}(h - \delta)\right]. \tag{8}$$

The KSC tower data were used again to evaluate the accuracy of Eq. (8). To simplify the analysis, the correction factors α and β were both set to one at first. Results, summarized in Table 5, are once again slightly dependent on the time zone. On average, the shear function is largely underpredicted by using Eq. (8), as the mean observed value of ρ_{h} was 2.8 and the mean calculated one was 1.8 (using 0700–1900 LST). The same was true at each individual tower for all pairs of 12-h-apart times. Again, the early-morning–late-afternoon pairs of hours (i.e., 0500–1700 through 0700–1900 LST) gave rise to larger values of the shear function than did all other pairs. For example, at tower 0403, the average observed value of ρ_h was 2.015, the average calculated value with the 0700–1900 LST pair was 1.864, and the average calculated value with the 0100–1300 LST pair was 1.761. The average behavior of ρ at all towers as a function of the 12-h-apart pairs of hours is shown in Fig. 10b. By using the correction factors $\alpha = 0.95$ and $\beta = 1.2$ [suggested in Archer and Jacobson (2004)], valid for the continental U.S. time zones (i.e., -5, -6, and -7 from UTC), the early-morning–late-afternoon effect was virtually eliminated. In fact, the average ρ obtained with correction factors at 0700–1900 LST was comparable to the average ρ obtained with other pairs of hours (Fig. 10b and Table 5).

The final question to investigate is how well the proposed formulation for the shear function actually mimics the real one. Figures 11a–c show examples of calculated and observed ρ_{h} at the tower closest to the average (0415), the tower with the worst performance (0001), and the tower with the best performance (0506), respectively. In general, the proposed sinusoidal pattern of ρ_h is a good approximation for the real pattern of the shear function. However, besides the general underestimation of the average value discussed above, the observed pattern shows a larger amplitude and a sharper transition from day to night (and from night to day). Also, the early-morning/late-afternoon hour pairs tend to produce a larger daily mean $\bar{\rho}$ than do other hour pairs. This supports the choice of the correction factors in Archer and Jacobson (2004), which forced a reduction of $\bar{\rho}$ ($\alpha < 1$) and an increase of A ($\beta > 1$).

4. Conclusions

In this study, the effects of interconnecting multiple wind farms through the transmission grid were investigated. The area of interest was within the midwestern United States, previously identified as one of the best locations for wind power harnessing over land. Nineteen sites with annual average wind speed at 80 m above ground, the hub height of modern wind turbines, greater than 6.9 m s^{-1} were identified and intercon-

TABLE 5. Values of observed and calculated ρ at two-level towers of the KSC network. The calculated values were obtained for all 12-h-apart pairs of sounding times. Values obtained with correction factors are also shown in the last column. In boldface are the average values of ρ observed and calculated at 0700–1900 LST, corresponding to 0000–1200 UTC in Florida, with and without correction factors.

		Sounding times (LST)											
Tower	Obs	0000–1200	0100–1300	0200–1400	0300–1500	0400–1600	0500–1700	0600–1800	0700–1900	0800–2000	0900–2100	1000–2200	1100–2300	0700–1900 LT corrected
0001	3.997	1.741	1.739	1.761	1.787	1.809	1.866	1.896	1.873	1.785	1.748	1.731	1.729	1.779
0108	3.210	1.752	1.743	1.753	1.771	1.783	1.807	1.845	1.825	1.772	1.763	1.754	1.756	1.735
0112	1.875	1.648	1.636	1.651	1.666	1.667	1.723	1.779	1.733	1.670	1.632	1.634	1.645	1.652
0211	2.215	1.581	1.577	1.604	1.621	1.640	1.753	1.741	1.790	1.679	1.670	1.638	1.609	1.697
0303	3.546	1.755	1.772	1.782	1.815	1.848	1.898	1.906	1.869	1.771	1.756	1.747	1.741	1.772
0311	1.862	1.618	1.614	1.628	1.642	1.662	1.732	1.780	1.751	1.669	1.635	1.617	1.626	1.663
0403	2.015	1.744	1.761	1.767	1.797	1.822	1.867	1.899	1.864	1.790	1.762	1.739	1.747	1.767
0412	3.310	1.620	1.615	1.632	1.651	1.672	1.766	1.811	1.756	1.651	1.629	1.608	1.618	1.671
0415	2.564	1.608	1.616	1.625	1.644	1.684	1.756	1.848	1.759	1.656	1.616	1.606	1.604	1.676
0506	1.813	1.693	1.695	1.689	1.711	1.694	1.719	1.742	1.724	1.704	1.673	1.685	1.681	1.641
0509	2.435	1.677	1.642	1.641	1.684	1.679	1.754	1.774	1.733	1.661	1.652	1.631	1.633	1.641
0714	3.318	1.630	1.614	1.642	1.663	1.741	1.743	1.828	1.748	1.662	1.631	1.620	1.636	1.661
0803	2.903	1.756	1.765	1.782	1.798	1.817	1.865	1.890	1.857	1.778	1.760	1.755	1.748	1.758
0805	3.408	1.662	1.642	1.714	1.691	1.730	1.756	1.808	1.745	1.671	1.659	1.671	1.655	1.652
Avg	**2.748**	1.678	1.674	1.691	1.710	1.732	1.786	1.825	**1.788**	1.709	1.685	1.674	1.673	**1.697**

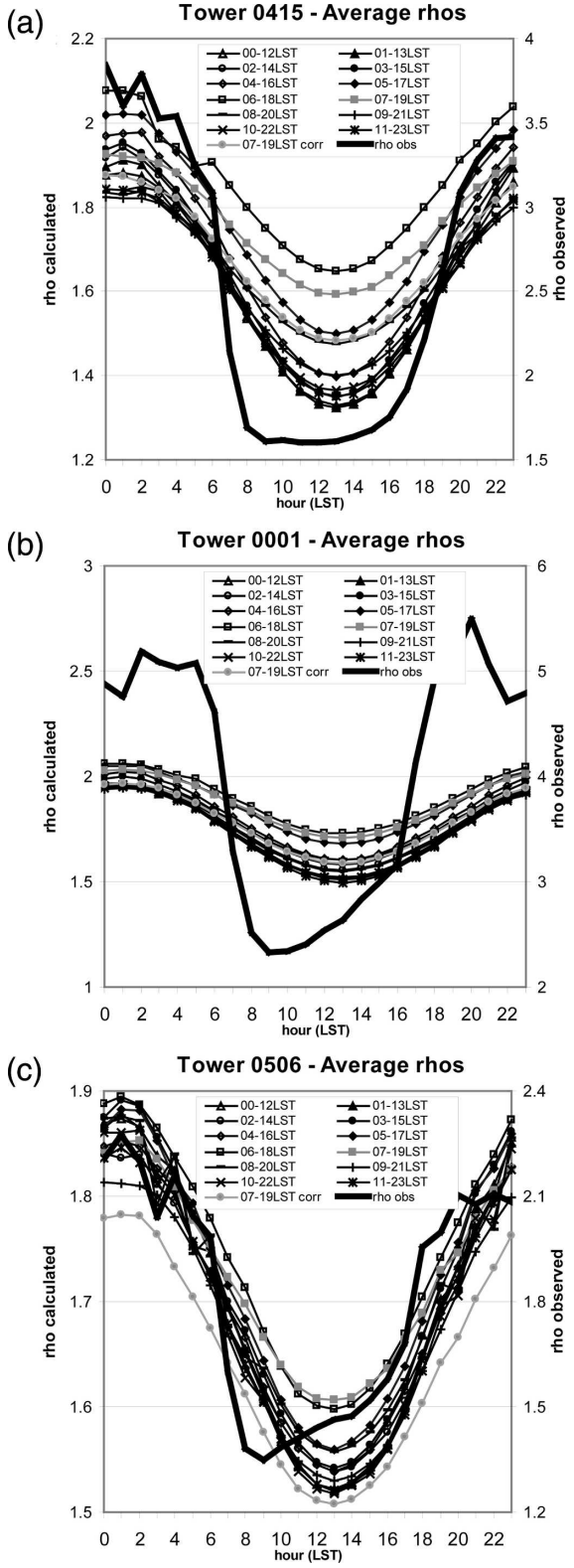

FIG. 11. Observed and calculated hourly ρ at (a) tower 0415 (closest to average), (b) tower 0001 (worst case), and (c) tower 0504 (best case). Note the different scales on axes.

nected within an increasingly larger array. Wind speeds at 80 m were calculated via the least squares method, which involved a combination of 10-m wind speed observations at the sites of interest and vertical wind profiles retrieved at nearby sounding stations. Observed data from the Kennedy Space Center in Florida were used to validate the method.

Array-average statistics were compared with those obtained from each individual site and from the same sites if they were not interconnected (linear sum). Parameters that depend linearly on the values at each individual site, such as array-average wind speed, wind power, and capacity factor, were unaffected by the interconnection, as expected. All other nonlinear parameters showed substantial improvements as the number of interconnected sites increased. These included standard deviations of array-average wind speed and wind power, which decreased as array size increased, array reliability, and reserve requirements, which decreased relative to both the linear sum and the total electricity delivered. The marginal benefit of each additional site decreased. However, no saturation of benefits was found, that is, positive marginal benefits were always found, even if small.

Contrary to common knowledge, an average of 33% and a maximum of 47% of yearly averaged wind power from interconnected farms can be used as reliable, baseload electric power. Equally significant, interconnecting multiple wind farms to a common point, and then connecting that point to a far-away city can allow the long-distance portion of transmission capacity to be reduced, for example, by 20% with only a 1.6% loss of energy.

Reliability was studied with the generation duration curve because it is relatively simple to implement and it does not require any load data. As such, the results described in this study are general and do not depend on the load. An alternative method to study reliability is the Effective Load Carrying Capability. Because of its complexity and dependency on load data, the ELCC approach is recommended for future studies.

In conclusion, this study implies that if interconnected wind is used on a large scale, a third or more of its energy can be used for reliable electric power and the remaining intermittent portion can be used for transportation (i.e., to power batteries or to produce hydrogen), allowing wind to solve energy, climate, and air pollution problems simultaneously.

Acknowledgments. We thank Prof. Willett Kempton for helpful comments and suggestions. This work was partially funded by the National Aeronautics and Space Administration.

REFERENCES

Ackermann, T., 2005: *Wind Power in Power Systems.* John Wiley and Sons, 691 pp.

Ahlstrom, M., L. Jones, R. Zavadil, and W. Grant, 2005: The future of wind forecasting and utility operations. *IEEE Power Energy Mag.,* **3,** 57–64.

American Wind Energy Association, cited 2004: Global wind energy market report. [Available online at http://www.awea.org/pubs/documents/globalmarket2004.pdf.]

Archer, C. L., and M. Z. Jacobson, 2003: Spatial and temporal distribution of U.S. winds and wind power at 80 m derived from measurements. *J. Geophys. Res.,* **108,** 4289, doi:10.1029/2002JD002076.

——, and ——, 2004: Corrections to "Spatial and temporal distribution of U.S. winds and wind power at 80 m derived from measurements." *J. Geophys. Res.,* **109,** D20116, doi:10.1029/2004JD005099.

——, and ——, 2005: Evaluation of global wind power. *J. Geophys. Res.,* **110,** D12110, doi:10.1029/2004JD005462.

——, and ——, 2006: Comments on "Evaluation of a wind power parameterization using tower observations." *J. Geophys. Res.,* **111,** D10103, doi:10.1029/2005JD006098.

Czisch, G., and B. Ernst, 2001: High wind power penetration by the systematic use of smoothing effects within huge catchment areas shown in a European example. *Proc. WINDPOWER 2001,* Washington, DC, American Wind Energy Association.

DeMeo, E. A., W. Grant, M. R. Milligan, and M. J. Schuerger, 2005: Wind plant integration. *IEEE Power Energy Mag.,* **3,** 38–46.

Energy Information Administration, cited 2004: International energy annual 2002. [Available online at http://www.eia.doe.gov/emeu/international/.]

Eriksen, P. B., T. Ackermann, H. Abildgaard, P. Smith, W. Winter, and J. R. García, 2005: System operation with high wind penetration. *IEEE Power Energy Mag.,* **3,** 65–74.

Forecast System Laboratory, 2004: Recent worldwide RAOB observations. CD-ROM. [Available online at http://www.fsl.noaa.gov/data/onlinedb.html.]

General Electric, 2004: 1.5sle/1.5sl/1.5s/1.5se wind turbines. 8 pp. [Available online at http://www.gewindenergy.com.]

Giebel, G., 2000: On the benefits of distributed generation of wind energy in Europe. Ph.D. thesis, Carl von Ossietzky Universität Oldenburg, 97 pp.

——, 2003: The state-of-the-art in short-term prediction of wind power: A literature overview. Project Anemos, Risø National Laboratory Tech. Rep., Roskilde, Denmark, 36 pp.

Holttinen, H., and R. Hirvonen, 2005: Power system requirements for wind power. *Wind Power in Power Systems,* T. Ackermann, Ed., John Wiley and Sons, 143–167.

International Energy Agency, 2003: Key World Energy Statistics 2003. International Energy Agency, Paris, France, 78 pp. [Available online at http://www.toplo-ruse.com/key2003.pdf.]

Jacobson, M. Z., and G. M. Masters, 2001: Exploiting wind versus coal. *Science,* **293,** 1438.

Kahn, E., 1979: The reliability of distributed wind generators. *Electric Power Syst. Res.,* **2,** 1–14.

Lazarus, S. M., and J. Bewley, 2005: Evaluation of a wind power parameterization using tower observations. *J. Geophys. Res.,* **110,** D07102, doi:10.1029/2004JD005614.

Masters, G. M., 2004: *Renewable and Efficient Electric Power Systems*. John Wiley and Sons, 654 pp.

Matevosyan, J., 2005: Wind power in areas with limited transmission capacity. *Wind Power in Power Systems,* T. Ackermann, Ed., John Wiley and Sons, 433–459.

Milligan, M. R., and R. Artig, 1998: Reliability benefits of dispersed wind resource development. National Renewable Energy Laboratory, NREL/CP-500-24314, Golden, CO, 11 pp.

——, and ——, 1999: Choosing wind power plant locations and sizes based on electric reliability measures using multiple-year wind speed measurements. National Renewable Energy Laboratory, NREL/CP-500-26724, Golden, CO, 9 pp.

——, and K. Porter, 2005: Determining the capacity value of wind: A survey of methods and implementation. National Renewable Energy Laboratory, NREL/CP-500-38062, Golden, CO, 30 pp.

National Climatic Data Center, 2004: Integrated surface hourly observations. CD-ROM. [Available online at http://ols.nndc.noaa.gov/plolstore/plsql/olstore.prodspecific?prodnum=C00353-CDR-S0001.]

Nørgård, P., G. Giebel, H. Holttinen, L. Söder, and A. Petterteig, 2004: Fluctuations and predictability of wind and hydropower. Project WILMAR, Risø National Laboratory Tech. Rep. R-1443(EN), Roskilde, Denmark, 72 pp.

North American Electric Reliability Council, cited 2005: 2000–2004 generating availability report. [Available online at http://www.nerc.com/~gads/.]

Piwko, R., D. Osborn, R. Gramlich, G. Jordan, D. Hawkins, and K. Porter, 2005: Wind energy delivery issues. *IEEE Power Energy Mag.,* **3,** 47–56.

Romanowitz, H. M., 2005: Wind power on weak grids in California and the US Midwest. *Wind Power in Power Systems,* T. Ackermann, Ed., John Wiley and Sons, 257–282.

Simonsen, T. K., and B. G. Stevens, 2004: Regional wind energy analysis for the Central United States. *Proc. Global Wind Power 2004,* Chicago, IL, American Wind Energy Association, 16 pp.

Zavadil, R., N. Miller, A. Ellis, and E. Muljadi, 2005: Making connections. *IEEE Power Energy Mag.,* **3,** 26–37.